

# Dynamic homogenization in periodic fibre reinforced media. Quasi-static limit for SH waves

W.J. Parnell \*, I.D. Abrahams

*School of Mathematics, University of Manchester, Oxford Road, Manchester M13 9PL, UK*

Received 4 August 2005; received in revised form 22 February 2006; accepted 7 March 2006

Available online 4 May 2006

---

## Abstract

The effective response of a periodic fibre reinforced material to SH wave propagation is studied using the method of asymptotic homogenization, complex variable theory and multipole expansions. The quasi-static limit of the effective properties is calculated when the wavelength is much longer than the defining lengthscale of the microstructure. The method developed allows the determination of the elastic properties in the most general (monoclinic) fibre reinforced media and the resulting expressions for the effective moduli are concise. The method is therefore both more general and provides neater closed form solutions than extant methods. Results are shown to be excellent even for very high volume fractions of fibres. © 2006 Elsevier B.V. All rights reserved.

*Keywords:* Asymptotic homogenization; SH waves; Quasi-statics; Monoclinic composites

---

## 1. Introduction

The subject of homogenization may be defined as the study of partial differential equations with rapidly oscillating coefficients. As a result of these oscillations, direct numerical solution is extremely difficult and it is therefore desirable to develop mathematical techniques to overcome these problems. Methods of homogenization date back to the end of the 19th century when various techniques were developed to find the *effective* or macroscopic response of inhomogeneous materials. In particular in [21] Rayleigh established his now well-known multipole method in order to find the effective electric properties of a periodic array of cylinders. More recently these methods have been extended to elasticity by McPhedran et al. [13,20,28] whose primary goal was to find the so called phononic band gaps of the periodic material. By taking the long wavelength limit, the effective properties may also be found. However such methods can exhibit problems with convergence for high volume fractions of fibres where estimates of the effective moduli become unreliable and special asymptotic techniques have to be called upon in order to solve the corresponding problem [14].

---

\* Corresponding author. Tel.: +161 2755809; fax: +161 2755819.  
E-mail address: [wparnell@maths.man.ac.uk](mailto:wparnell@maths.man.ac.uk) (W.J. Parnell).

We are interested in developing a reliable and relatively straightforward technique for calculating the effective dynamic elastic properties of a periodic fibre reinforced medium (of arbitrary geometry and volume fraction, so that fibres which are close to touching are included) when excited by a long wavelength plane wave. Knowledge of such effective properties is essential for models of composite materials in engineering applications. The statics problem has been well studied by the method of asymptotic homogenization (MAH) [2], [19]. This method exploits the scales involved in the problem by posing asymptotic expansions in powers of  $\epsilon$ , the ratio of micro to macroscale in the material and relies on the material having periodic structure. Meguid and Kalamkarov [15] used the technique to find the effective static properties of a tetragonal fibre reinforced material using Weierstrassian elliptic functions in order to account for the periodic behaviour. In a series of papers Sabina et al. [23,22] and references therein solved static problems using the MAH for materials of various simple symmetries and for materials where the phases are permitted to be transversely isotropic. They also pointed out several errors in the article of Meguid and Kalamkarov [15]. Again, Weierstrassian elliptic functions were employed. The MAH is not restricted to problems in elasticity as may be seen by its applications to viscoelasticity by Yi et al. [27], thermoelasticity by Francfort [4] and Parnell [18] and many more, see Rodriguez-Ramos et al. [22]. Nemat-Nasser et al. [16,8] developed the method of equivalent inclusions for periodic media using the notion of eigenstrain and Fourier Series expansions. This method was applied to fibre reinforced media by Jiang et al. [10].

In contrast to the above we are interested in the effective (low frequency) *dynamic* response of a periodic fibre reinforced material. This problem is more appealing than its static counterpart since for an unbounded material there are two natural lengthscales in the problem, the microscale ( $O(q)$ ) defining fluctuations on the scale of the microstructure and the macroscale ( $O(1/k_0)$ ) where  $k_0$  is the wavenumber in the host material. This allows us to define the (physically meaningful) small parameter  $qk_0 = \epsilon \ll 1$  and we can use the MAH in the dynamic context, posing asymptotic expansions in powers of  $\epsilon$ . The leading order term corresponds to the quasi-static limit where no dispersive effects result. This term should be numerically identical to extant methods in static homogenization. In the dynamic case, higher order terms have physical significance (dispersion) whereas for statics this is not the case – the method only makes sense in the strict limit as  $\epsilon \rightarrow 0$  since  $\epsilon$  is an artificial parameter (no macro lengthscale exists for an unbounded material in statics) and thus the dynamic approach is preferable.

We report on the leading order term here for materials with various structure, leaving the next order dispersive effects for a later article. We note however that the resulting closed form solutions are considerably simpler than those reported by Meguid et al. [15] and Sabina et al. [23]. This is primarily because we do not appeal directly to the theory of Weierstrassian elliptic functions when formulating the necessary doubly periodic functions. The dynamic approach allows more complex material behaviour to be identified (i.e. dispersive effects) and furthermore the flexibility and simplicity of the doubly periodic basis functions to be defined at the end of Section 4, permits extremely complicated structures to be modelled with little extra difficulty as we shall show.

The analysis to follow thereby allows the materials to possess the most general symmetry possible for fibre reinforced media; i.e. monoclinicity, corresponding to a material with only one plane of material symmetry and 13 elastic constants. In this article we focus on the scalar SH wave problem which allows 3 of these constants to be determined. The coupled P and SV wave problem will follow shortly. The materials are built up from *periodic cells* which tessellate the entire  $xy$  plane. These periodic cells may have quite general structure as we shall show. The only restriction on the cells is that their defining lengthscale ( $q$ ) must be such that the condition  $qk_0 = \epsilon \ll 1$  is retained.

On finding the quasi-static limit we compare our results with those of various static homogenization methods. In particular we can check that the results lie within the well-known Hashin Shtrikman bounds [7]. Furthermore for particular geometries even better energy bounds can be derived [6] and our exact solutions must lie within these. Various self-consistent methods have been proposed for the purposes of dynamic homogenization [11,24]. These methods approximate the displacements within the inclusion as if it experienced an effective field. The effective *medium* and effective *field* self-consistent schemes [11] estimate this as the field which would occur if the fibres were embedded in the effective material or host material, respectively, and the incoming wave was the effective wave in both cases. Thus, the method requires the solution of a single scattering problem which for periodic materials becomes rather difficult since for example in an effective orthotropic

medium, one must surround the inclusion with an orthotropic material. Due to the use of this single scattering problem, the method relies on one to *guess* the symmetry of the resulting anisotropic material whereas with other methods this arises naturally.

Finally we mention the  $T$ -matrix method [26] which attempts to incorporate interactions between fibres in a random material. This method has the capability for statistics to be introduced into the analysis (i.e. correlation functions). The quasi-static limit of the  $T$ -matrix result in the *well stirred* limit corresponds exactly to the special result of Hashin [6] when a particular limit, corresponding to “no gaps between composite cylinders” is taken [6]. This method also gives the same results as the effective field self-consistent scheme discussed above.

In Section 2 we set up the problem, introduce the Method of Asymptotic Homogenization and explain how it is applied. In Section 3 we find the homogenized equation for the leading order term of the displacement by appealing to periodicity properties. In order to find the effective elastic constants, we must solve the problem at  $O(\epsilon)$  and this is done in Section 4 by constructing a doubly periodic function which will satisfy the necessary boundary conditions. This is then used as a building block for materials with specific geometries in Section 5 where the fibres have circular cross section. More general cross sections are considered in Section 6 and we apply the method to fibres of elliptic cross section. Finally in Section 7 we conclude by reviewing the work and indicating where we should proceed from here.

## 2. SH waves in a monoclinic material

We work in Cartesian coordinates where the  $z$  axis is parallel to the fibres. Consider the case of SH waves propagating in the  $xy$  plane, polarized along the  $z$  axis. Since no mode conversion results at the fibre/host interface this is a scalar problem [5]. The cross section of the material in the  $xy$  plane is defined by a periodic cell which tessellates the entire plane, examples of which are shown in Fig. 1. We see that these cells can become extremely general allowing complicated structures to be considered and reference to Fig. 1(a), shows that there may be more than one fibre in each periodic cell. The location of the  $(s, t)$ th periodic cell is defined by its lattice vector  $\mathbf{R}(s, t)$  as follows:

$$\mathbf{R}(s, t) = q(s\mathbf{l}_1 + t\mathbf{l}_2), \quad s, t \in \mathbb{Z}, \quad (2.1)$$

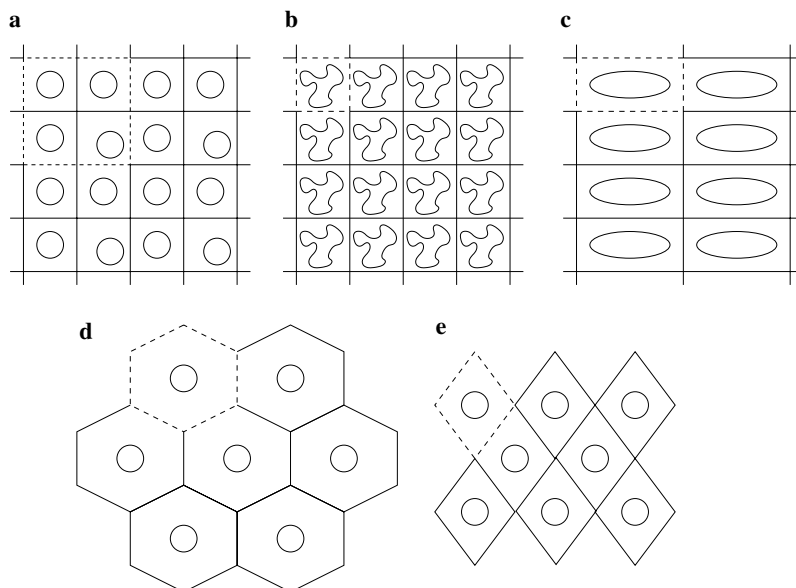


Fig. 1. Examples of cross sections in the  $xy$  plane – the dashed lines enclose a periodic cell. (a and b) Show examples of monoclinic materials. In (a) the monoclinicity is caused by the perturbation of one of the fibres in the periodic cell off the square (tetragonal) lattice. In (b) it is caused by the irregular shape of the fibres. (c) Shows an example of an orthotropic material. In (d and e) we see hexagonal and rhombic symmetry, respectively.

so that  $q$  is the characteristic lengthscale of the periodic cell (and thus the microstructure) and  $\mathbf{l}_1, \mathbf{l}_2 \in \mathbb{R} \times \mathbb{R}$  are vectors whose components are  $O(1)$ . Thus for a square lattice (tetragonal symmetry, corresponding to 6 elastic constants) one would choose

$$\mathbf{l}_1 = (1, 0), \quad \mathbf{l}_2 = (0, 1). \tag{2.2}$$

The most general fibre reinforced material is monoclinic and the corresponding elastic moduli tensor  $C_{ijkl}$  relating stress to strain, has one plane of reflectional symmetry (in this case the  $xy$  plane) and 13 independent components [12]. The SH wave relates to antiplane motion and thus requires consideration of Hooke’s law for a monoclinic material in such a deformation [12]:

$$\sigma_{13} = 2C_{1313}e_{13} + 2C_{1323}e_{23}, \tag{2.3}$$

$$\sigma_{23} = 2C_{2313}e_{13} + 2C_{2323}e_{23}, \tag{2.4}$$

where  $\sigma_{13}$  and  $\sigma_{23}$  are the (tensorial) shear stresses and  $e_{13}$  and  $e_{23}$  are the (tensorial) shear strains. We also note the symmetries of the elastic moduli tensor,  $C_{ijkl} = C_{jikl} = C_{ijlk} = C_{klij}$ , so that  $C_{1323} = C_{2313}$ . Thus, analysis of the SH wave allows us to determine *three* of the 13 effective moduli. Alternatively (2.3) and (2.4) may be written in the engineering notation [25]

$$\tau_4 = c_{44}\gamma_4 + c_{45}\gamma_5, \tag{2.5}$$

$$\tau_5 = c_{45}\gamma_4 + c_{55}\gamma_5, \tag{2.6}$$

where  $\tau_4 = \sigma_{23}$  and  $\tau_5 = \sigma_{13}$  are the engineering shear stresses and  $\gamma_4 = 2e_{23}, \gamma_5 = 2e_{13}$  are the engineering shear strains. Thus we conclude in this notation that  $c_{44} = C_{2323}, c_{45} = C_{1323} = C_{2313}$  and  $c_{55} = C_{1313}$ .

In Fig. 2 we see an example of the class of composite materials we are modelling together with relevant notation. In general we consider a periodic cell comprising an isotropic host phase of density  $\rho_0$  and shear modulus  $\mu_0$  and  $N$  isotropic fibres of arbitrary shape having densities  $\rho_i$  and shear moduli  $\mu_i$ , ( $1 \leq i \leq N$ ). For the SH problem, given time harmonic behaviour  $\exp(-i\omega t)$ , the displacement in the  $z$  direction, denoted by  $w = w(x, y) = w(\mathbf{x})$  satisfies the scalar Helmholtz equation:

$$\nabla^2 w(\mathbf{x}) + k_0^2 \alpha^2(\mathbf{x}) w(\mathbf{x}) = 0, \tag{2.7}$$

where

$$\alpha(\mathbf{x}) = \begin{cases} 1 & \text{if } x \in D_0, \\ \alpha_i = k_i/k_0 & \text{if } x \in D_i \end{cases} \tag{2.8}$$

and the domains of the  $i$ th fibre and host within the periodic cell are denoted by  $D_i$  and  $D_0$ , respectively. Furthermore,

$$k_0^2 = \frac{\omega^2 \rho_0}{\mu_0}, \quad k_i^2 = \frac{\omega^2 \rho_i}{\mu_i}, \tag{2.9}$$

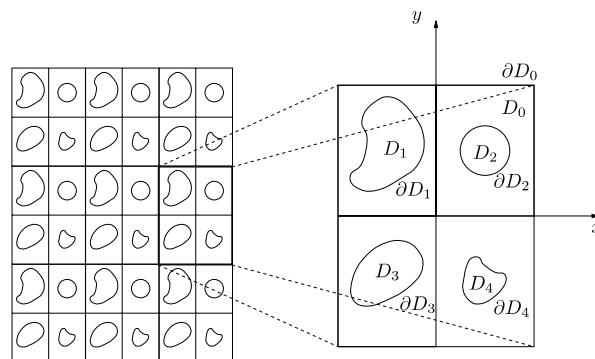


Fig. 2. A cross section of a monoclinic material with a periodic cell containing four inclusions. Each inclusion may possess distinct elastic properties.

and thus

$$\alpha_i^2 = \frac{k_i^2}{k_0^2} = \frac{d_i}{m_i} = O(1), \quad (2.10)$$

where  $d_i = \rho_i/\rho_0$  and  $m_i = \mu_i/\mu_0$ . On non-dimensionalizing lengthscales on  $q$ , (2.7) becomes

$$\nabla^2 w(\mathbf{x}) + \epsilon^2 \alpha^2(\mathbf{x}) w(\mathbf{x}) = 0, \quad (2.11)$$

where  $\epsilon = qk_0 \ll 1$  is the small parameter in the problem, reflecting the relationship between the microscale  $q$  and macroscale  $1/k_0$ . The non-dimensionalized lattice vector is

$$\mathbf{R}(s, t) = s\mathbf{l}_1 + t\mathbf{l}_2, \quad s, t \in \mathbb{Z} \quad (2.12)$$

and non-dimensionalized boundary conditions of continuity of displacement and normal stress on the boundary  $\partial D_i$  of the  $i$ th fibre require

$$w|_{\partial D_i^+} = w|_{\partial D_i^-}, \quad (2.13)$$

$$\mathbf{n}_i \cdot \nabla w|_{\partial D_i^+} = m_i \mathbf{n}_i \cdot \nabla w|_{\partial D_i^-}, \quad (2.14)$$

for each  $i$ , where  $\mathbf{n}_i$  is the normal to the boundary  $\partial D_i$  of the  $i$ th fibre. We introduce the two independent lengthscales,

$$\mathbf{x} = \boldsymbol{\xi}, \quad \mathbf{x} = \frac{1}{L(\epsilon)} \mathbf{z}, \quad (2.15)$$

where  $L(\epsilon)$  is some expansion in  $\epsilon$ , tending to zero as  $\epsilon \rightarrow 0$  in a manner to be discussed below, so that  $\boldsymbol{\xi}$  and  $\mathbf{z}$  are *short* and *long* lengthscales, respectively. The displacement is now a function of the two *independent* variables  $\boldsymbol{\xi}$  and  $\mathbf{z}$ :

$$w = w(\boldsymbol{\xi}, \mathbf{z}). \quad (2.16)$$

Let us suppose that we can expand the displacement and  $L(\epsilon)$  in asymptotic expansions of the form<sup>1</sup>

$$w(\boldsymbol{\xi}, \mathbf{z}) = w_0(\boldsymbol{\xi}, \mathbf{z}) + \epsilon w_1(\boldsymbol{\xi}, \mathbf{z}) + O(\epsilon^2), \quad (2.17)$$

$$L(\epsilon) = \epsilon + L_2 \epsilon^2 + L_3 \epsilon^3 + O(\epsilon^4). \quad (2.18)$$

Introducing these expansions into (2.11) and noting that

$$\nabla_{\mathbf{x}} = \nabla_{\boldsymbol{\xi}} + L(\epsilon) \nabla_{\mathbf{z}} \quad (2.19)$$

we obtain

$$\left[ \nabla_{\boldsymbol{\xi}}^2 + 2\epsilon \nabla_{\boldsymbol{\xi}} \cdot \nabla_{\mathbf{z}} + \epsilon^2 (2L_2 \nabla_{\boldsymbol{\xi}} \cdot \nabla_{\mathbf{z}} + \nabla_{\mathbf{z}}^2) + \epsilon^3 (2L_3 \nabla_{\boldsymbol{\xi}} \cdot \nabla_{\mathbf{z}} + 2L_2 \nabla_{\mathbf{z}}^2) + \cdots + \alpha^2(\boldsymbol{\xi}) \epsilon^2 \right] (w_0 + \epsilon w_1 + \epsilon^2 w_2 + \cdots) = 0. \quad (2.20)$$

If we do the same with the boundary conditions (2.13) and (2.14) we find that

$$(w_0 + \epsilon w_1 + \epsilon^2 w_2 + \cdots)|_{\partial D_i^+} = (w_0 + \epsilon w_1 + \epsilon^2 w_2 + \cdots)|_{\partial D_i^-}, \quad (2.21)$$

$$\begin{aligned} \mathbf{n}_i \cdot (\nabla_{\boldsymbol{\xi}} + (\epsilon + L_2 \epsilon^2 + \cdots) \nabla_{\mathbf{z}}) (w_0 + \epsilon w_1 + \epsilon^2 w_2 + \cdots)|_{\partial D_i^+} \\ = m_i \mathbf{n}_i \cdot (\nabla_{\boldsymbol{\xi}} + (\epsilon + L_2 \epsilon^2 + \cdots) \nabla_{\mathbf{z}}) (w_0 + \epsilon w_1 + \epsilon^2 w_2 + \cdots)|_{\partial D_i^-}. \end{aligned} \quad (2.22)$$

Furthermore we exploit the fact that we have introduced two lengthscales by requiring that each  $w_j$  should be doubly periodic with respect to the short lengthscale  $\boldsymbol{\xi}$ , i.e.

$$w_j(\boldsymbol{\xi}, \mathbf{z}) = w_j(\boldsymbol{\xi} + \mathbf{R}(s, t), \mathbf{z}) \quad (2.23)$$

<sup>1</sup> We assume expansions in powers of  $\epsilon$  remaining aware that we may actually require terms of the order  $\epsilon^m \log^n \epsilon$ .

for each  $j$  and for any  $s, t \in \mathbb{Z}$ . Thus, we can solve the problem at each order by equating terms of equal powers in  $\epsilon$ . At leading order we obtain the governing equation

$$\nabla_{\xi}^2 w_0 = 0 \tag{2.24}$$

together with the boundary conditions

$$w_0|_{\partial D_i^+} = w_0|_{\partial D_i^-}, \tag{2.25}$$

$$\mathbf{n}_i \cdot \nabla_{\xi} w_0|_{\partial D_i^+} = m_i \mathbf{n}_i \cdot \nabla_{\xi} w_0|_{\partial D_i^-} \tag{2.26}$$

and the double periodicity condition (2.23) for  $j = 0$ . The solution at this leading order must be

$$w_0(\xi, \mathbf{z}) = A(\mathbf{z}). \tag{2.27}$$

As is always the case [2], we see that the leading order solution does not depend *explicitly* upon the short lengthscale  $\xi$ . A doubly periodic function of  $\xi$ , satisfying Laplace’s equation cannot also satisfy boundary condition (2.26) and thus the solution must be a function of the macroscale variable  $\mathbf{z}$  alone.

At  $O(\epsilon)$ , on using (2.27) we find that the governing equation is

$$\nabla_{\xi}^2 w_1 = 0. \tag{2.28}$$

The associated boundary conditions are

$$w_1|_{\partial D_i^+} = w_1|_{\partial D_i^-}, \tag{2.29}$$

$$\mathbf{n}_i \cdot \nabla_{\xi} w_1|_{\partial D_i^+} - m_i \mathbf{n}_i \cdot \nabla_{\xi} w_1|_{\partial D_i^-} = (m_i - 1) \mathbf{n}_i \cdot \nabla_{\mathbf{z}} A(\mathbf{z}) \tag{2.30}$$

and we require the double periodicity condition (2.23) with  $j = 1$ . In order to continue we define the vector functions  $\mathbf{W}(\xi)$  and  $\mathbf{W}^i(\xi)^2$  such that

$$w_1(\xi, \mathbf{z}) = \begin{cases} \mathbf{W}(\xi) \cdot \nabla_{\mathbf{z}} A(\mathbf{z}) + B(\mathbf{z}), & \xi \in D_0, \\ \mathbf{W}^i(\xi) \cdot \nabla_{\mathbf{z}} A(\mathbf{z}) + B^i(\mathbf{z}), & \xi \in D_i, \end{cases} \tag{2.31}$$

where  $B(\mathbf{z})$  and  $B^i(\mathbf{z})$  are yet to be determined. This form enables the separation of the variables  $\xi$  and  $\mathbf{z}$  in the solution scheme. From (2.28), we obtain

$$\nabla_{\xi}^2 \mathbf{W}(\xi) = 0, \quad \xi \in D_0, \tag{2.32}$$

$$\nabla_{\xi}^2 \mathbf{W}^i(\xi) = 0 \quad \xi \in D_i \tag{2.33}$$

and boundary condition (2.29) yields

$$B^i(\mathbf{z}) = B(\mathbf{z}), \tag{2.34}$$

$$\mathbf{W}(\xi)|_{\partial D_i} = \mathbf{W}^i(\xi)|_{\partial D_i}. \tag{2.35}$$

The second boundary condition (2.30) implies that

$$\mathbf{n}_i \cdot \nabla_{\xi} (\mathbf{W} - m_i \mathbf{W}^i)|_{\partial D_i} = (m_i - 1) \mathbf{n}_i|_{\partial D_i} \tag{2.36}$$

where  $\nabla_{\xi} \mathbf{W}$  is a second order tensor. Therefore, we have reduced the problem at  $O(\epsilon)$  to the calculation of doubly periodic vector functions  $\mathbf{W}$  and  $\mathbf{W}^i$ , analytic in their respective domains satisfying the boundary conditions (2.35) and (2.36).

### 3. The homogenized equation

We shall now show how the governing equation for  $A(\mathbf{z})$  is derived from the  $O(\epsilon^2)$  problem. From this equation, the quasi-static effective moduli may be found in terms of the solution to the  $O(\epsilon)$  problem. This

<sup>2</sup> Note that the superscript  $i$  denotes that the function refers to the  $i$ th inclusion; it is not a power.

reveals that although the leading order solution does not *explicitly* depend on  $\xi$ , it does have *implicit* dependence as a result of the coefficients in its governing equation. At  $O(\epsilon^2)$  the governing equation is

$$\nabla_{\xi}^2 w_2 + 2(\nabla_{\xi} \cdot \nabla_{\mathbf{z}})(w_1 + L_2 w_0) + \nabla_{\mathbf{z}}^2 w_0 + \alpha^2(\xi)w_0 = 0 \tag{3.1}$$

subject to continuity of the displacement on  $\partial D_i$  and the continuity of normal stress boundary condition

$$\mathbf{n}_i \cdot (\nabla_{\xi} w_2 + \nabla_{\mathbf{z}}(w_1 + L_2 w_0)) \Big|_{\partial D_i^+} = m_i \mathbf{n}_i \cdot (\nabla_{\xi} w_2 + \nabla_{\mathbf{z}}(w_1 + L_2 w_0)) \Big|_{\partial D_i^-}. \tag{3.2}$$

Since  $w_0$  is a function of  $\mathbf{z}$  only, (3.1) can be written as

$$\nabla_{\xi} \cdot (\nabla_{\xi} w_2 + \nabla_{\mathbf{z}}(w_1 + L_2 w_0)) = -\nabla_{\xi} \cdot \nabla_{\mathbf{z}} w_1 - \nabla_{\mathbf{z}}^2 w_0 - \alpha^2(\xi)w_0. \tag{3.3}$$

Integrating this over  $D_0$ , invoking Green’s Theorem and imposing the periodicity conditions we obtain

$$\sum_{i=1}^N \int_{\partial D_i^+} (\nabla_{\xi} w_2 + \nabla_{\mathbf{z}}(w_1 + L_2 w_0)) \cdot \mathbf{n}_i \, dl = \int_{D_0} (\nabla_{\xi} \cdot \nabla_{\mathbf{z}} w_1 + \nabla_{\mathbf{z}}^2 w_0 + w_0) \, d\xi. \tag{3.4}$$

If we apply a similar procedure to *each* interior domain of the fibres  $D_i$  within the periodic cell, multiply by  $m_i$  and sum these equations, we obtain the expression

$$-\sum_{i=1}^N m_i \int_{\partial D_i^-} (\nabla_{\xi} w_2 + \nabla_{\mathbf{z}}(w_1 + L_2 w_0)) \cdot \mathbf{n}_i \, dl = \sum_{i=1}^N m_i \int_{D_i} (\nabla_{\xi} \cdot \nabla_{\mathbf{z}} w_1 + \nabla_{\mathbf{z}}^2 w_0 + \alpha_i^2 w_0) \, d\xi. \tag{3.5}$$

Integrating the boundary condition (3.2) around each  $\partial D_i$  in the periodic cell and summing these equations, invoking (3.4), (3.5), and the solution  $w_0 = A(\mathbf{z})$ , together with (2.31), we obtain the *homogenized wave equation*

$$\left\{ \left( |D_0| + \sum_{i=1}^N m_i |D_i| \right) \nabla_{\mathbf{z}}^2 + \nabla_{\mathbf{z}} \cdot \left( \mathbf{H}_e + \sum_{i=1}^N m_i \mathbf{H}_i \right) \cdot \nabla_{\mathbf{z}} + \left( |D_0| + \sum_{i=1}^N d_i |D_i| \right) \right\} A(\mathbf{z}) = 0, \tag{3.6}$$

where  $\mathbf{H}_i$  and  $\mathbf{H}_e$  are second order tensors defined by:

$$\mathbf{H}_i = \int_{D_i} \nabla_{\xi} \mathbf{W}^i \, d\xi = \int_{\partial D_i} \mathbf{W}^i \cdot \mathbf{n}_i \, dl = |D_i| \begin{pmatrix} H_{11}^i & H_{12}^i \\ H_{21}^i & H_{22}^i \end{pmatrix}, \tag{3.7}$$

$$\mathbf{H}_e = \int_{D_0} \nabla_{\xi} \mathbf{W} \, d\xi = -\sum_{i=1}^n \int_{\partial D_i} \mathbf{W}^i \cdot \mathbf{n}_i \, dl = -\sum_{i=1}^n \mathbf{H}_i \tag{3.8}$$

and  $|D_0|$  and  $|D_i|$  denote the cross-sectional areas of the domains  $D_0$  and  $D_i$ , respectively. Expression (3.8) allows us to write the homogenized wave equation more concisely as

$$\left\{ \left( |D_0| + \sum_{i=1}^N m_i |D_i| \right) \nabla_{\mathbf{z}}^2 + \sum_{i=1}^N (m_i - 1) \nabla_{\mathbf{z}} \cdot \mathbf{H}_i \cdot \nabla_{\mathbf{z}} + \left( |D_0| + \sum_{i=1}^N d_i |D_i| \right) \right\} A(\mathbf{z}) = 0 \tag{3.9}$$

and we now see what was indicated earlier, the implicit dependence of  $A(\mathbf{z})$  on the short lengthscale by virtue of the appearance of the tensor  $\mathbf{H}_i$  as a coefficient in the homogenized equation, accounting for the anisotropy of different geometries. Dividing (3.9) by the total cross-sectional area of the periodic cell  $|D|$ , the homogenized equation takes the form

$$\left( \mathcal{A} \frac{\partial^2}{\partial z_1^2} + \mathcal{B} \frac{\partial^2}{\partial z_2^2} + \mathcal{C} \frac{\partial^2}{\partial z_1 \partial z_2} + \mathcal{D} \right) A(\mathbf{z}) = 0, \tag{3.10}$$

where

$$\mathcal{A} = \phi_0 + \sum_{i=1}^N \phi_i(m_i + (m_i - 1)H_{11}^i), \tag{3.11}$$

$$\mathcal{B} = \phi_0 + \sum_{i=1}^N \phi_i(m_i + (m_i - 1)H_{22}^i), \tag{3.12}$$

$$\mathcal{C} = \sum_{i=1}^N \phi_i(m_i - 1)(H_{12}^i + H_{21}^i), \tag{3.13}$$

$$\mathcal{D} = \phi_0 + \sum_{i=1}^N \phi_i d_i \tag{3.14}$$

and  $\phi_0, \phi_i$  are the volume fractions of host and the  $i$ th fibre, respectively;

$$\phi_0 = \frac{|D_0|}{|D|}, \quad \phi_i = \frac{|D_i|}{|D|}, \quad |D| = |D_0| + \sum_{i=1}^N |D_i|. \tag{3.15}$$

Plane wave solutions to (3.10) with wavenumber  $\hat{\alpha}_*$  (scaled on  $k_0$ ) must take the form

$$A(\mathbf{z}) = \hat{A} \exp(i\hat{\alpha}_*(\Theta)\mathbf{v}_i z_i), \tag{3.16}$$

where the direction of propagation in the  $xy$  plane is defined by  $\mathbf{v} = (\cos\Theta, \sin\Theta)$ . On substituting this into (3.10) we find that for solutions of this form to exist we must have

$$\hat{\alpha}_*^2(\Theta) = \frac{\mathcal{D}}{\mathcal{A} \cos^2 \Theta + \mathcal{B} \sin^2 \Theta + \mathcal{C} \sin \Theta \cos \Theta}. \tag{3.17}$$

At this point if we scale back to  $\mathbf{x}$  coordinates using (2.15) we find that

$$\hat{\alpha}_* \mathbf{v}_i z_i = \hat{\alpha}_* L(\epsilon) \mathbf{v}_i x_i \tag{3.18}$$

$$= \alpha_* \mathbf{v}_i x_i, \tag{3.19}$$

so that the effective wave number  $\alpha_*$  (again scaled on  $k_0$ ) is defined by

$$\alpha_*^2(\Theta) = (\hat{\alpha}_* L(\epsilon))^2 \tag{3.20}$$

$$= \hat{\alpha}_*^2 \epsilon^2 + O(\epsilon^3) \tag{3.21}$$

$$= \frac{\mathcal{D} \epsilon^2}{\mathcal{A} \cos^2 \Theta + \mathcal{B} \sin^2 \Theta + \mathcal{C} \sin \Theta \cos \Theta} + O(\epsilon^3), \tag{3.22}$$

where  $\epsilon$  may be interpreted as a non-dimensionalized frequency. It is easily shown using (2.3) and (2.4) that a *homogeneous* monoclinic material (propagating at the non-dimensionalized frequency  $\epsilon$ ) with material properties  $d_*$  (scaled on  $\rho_0$ ) and  $C_{1313}^*, C_{2323}^*$  and  $C_{1323}^*$  (scaled on  $\mu_0$ ), responds with wavenumber

$$\alpha_{\text{hom}}^2(\Theta) = \frac{d_* \epsilon^2}{C_{1313}^* \cos^2 \Theta + C_{2323}^* \sin^2 \Theta + 2C_{1323}^* \sin \Theta \cos \Theta}. \tag{3.23}$$

Therefore on writing  $\phi_0 = 1 - \phi_1 - \phi_2 - \dots - \phi_N$  we can read off the *quasi-static* effective moduli by comparing (3.22) with (3.23) and identify them as

$$d^* = \mathcal{D} = 1 + \sum_{i=1}^N \phi_i(d_i - 1), \tag{3.24}$$

$$C_{1313}^* = m_x^* = \mathcal{A} = 1 + \sum_{i=1}^N \phi_i(m_i - 1)(1 + H_{11}^i), \tag{3.25}$$

$$C_{2323}^* = m_y^* = \mathcal{B} = 1 + \sum_{i=1}^N \phi_i(m_i - 1)(1 + H_{22}^i), \tag{3.26}$$

$$C_{1323}^* = m_{xy}^* = \frac{1}{2} \mathcal{C} = \frac{1}{2} \sum_{i=1}^N \phi_i (m_i - 1) (H_{12}^i + H_{21}^i). \quad (3.27)$$

Thus we interpret  $d_*$  as the effective density,  $m_x^*$  and  $m_y^*$  as the effective shear moduli relating to shearing on planes perpendicular to the  $x$  and  $y$  axes, respectively, and  $m_{xy}^*$  as the cross modulus relating to additional shear stresses resulting from the shear strain in a perpendicular direction (e.g. the contribution of  $e_{23}$  to  $\sigma_{13}$ ; see (2.3)). From hereon in we will be solely concerned with fibres having circular cross section (i.e.  $\mathbf{n}_i = (\cos\theta_i, \sin\theta_i)$ ) for  $\theta_i$  centred at the origin of each fibre) with the exception of Section 6 where more general fibre cross sections will be considered and results are computed for elliptical cross sections.

#### 4. The $O(\epsilon)$ problem

As discussed in the previous section, at  $O(\epsilon)$  we seek doubly periodic solutions  $\mathbf{W}$  and  $\mathbf{W}^i$  which are analytic in their respective domains and for circular fibres satisfy the boundary conditions

$$\mathbf{W}(\xi)|_{r=r_i} = \mathbf{W}^i(\xi)|_{r=r_i}, \quad (4.1)$$

$$\frac{\partial}{\partial r} (\mathbf{W} - m_i \mathbf{W}^i) \Big|_{r=r_i} = (m_i - 1) (\cos \theta, \sin \theta) \Big|_{r=r_i}, \quad (4.2)$$

where  $r = r_i$  is the radius of the  $i$ th fibre. We have introduced the local polar coordinate system  $(r, \theta)$  which has its origin at the centre of the  $i$ th fibre cross section.<sup>3</sup> Therefore inside the  $i$ th fibre, we may pose a solution of the form  $\mathbf{W}^i = (W_1^i, W_2^i)$  where

$$W_1^i = a_0^i + \sum_{m=1}^{\infty} \{ a_m^i r^m \cos m\theta + b_m^i r^m \sin m\theta \}, \quad (4.3)$$

$$W_2^i = \hat{a}_0^i + \sum_{m=1}^{\infty} \{ \hat{a}_m^i r^m \cos m\theta + \hat{b}_m^i r^m \sin m\theta \} \quad (4.4)$$

and  $a_n^i, \hat{a}_n^i, b_n^i, \hat{b}_n^i \in \mathbb{R}$  and a *local solution* valid in some neighbourhood outside the  $i$ th fibre may take the form  $\mathbf{W} = (Y_1^i, Y_2^i)$  where

$$Y_1^i = c_0^i + \sum_{m=1}^{\infty} \left\{ \left( c_m^i r^m + \frac{c_{-m}^i}{r^m} \right) \cos m\theta + \left( d_m^i r^m - \frac{d_{-m}^i}{r^m} \right) \sin m\theta \right\}, \quad (4.5)$$

$$Y_2^i = \hat{c}_0^i + \sum_{m=1}^{\infty} \left\{ \left( \hat{c}_m^i r^m + \frac{\hat{c}_{-m}^i}{r^m} \right) \cos m\theta + \left( \hat{d}_m^i r^m - \frac{\hat{d}_{-m}^i}{r^m} \right) \sin m\theta \right\} \quad (4.6)$$

and  $c_n^i, \hat{c}_n^i, d_n^i, \hat{d}_n^i \in \mathbb{R}$ . The superscripts  $i$  denote that this is a solution local to the  $i$ th fibre. The full doubly periodic solution outside the fibres will be some superposition of these, as we shall see shortly. Imposing (4.1) we obtain the relations

$$a_0^i = c_0^i, \quad (4.7)$$

$$\hat{a}_0^i = \hat{c}_0^i, \quad (4.8)$$

$$a_n^i = c_n^i + c_{-n}^i r_i^{-2n}, \quad n \geq 1, \quad (4.9)$$

$$\hat{a}_n^i = \hat{c}_n^i + \hat{c}_{-n}^i r_i^{-2n}, \quad n \geq 1, \quad (4.10)$$

$$b_n^i = d_n^i + d_{-n}^i r_i^{-2n}, \quad n \geq 1, \quad (4.11)$$

$$\hat{b}_n^i = \hat{d}_n^i + \hat{d}_{-n}^i r_i^{-2n}, \quad n \geq 1 \quad (4.12)$$

and from (4.2) we obtain

<sup>3</sup> Strictly the local polar coordinate system of the  $i$ th fibre should be referred to with an index (say  $i$ ) but to avoid complicated notation this is not followed and should not cause confusion.

$$(c_1^i - c_{-1}^i r_i^{-2}) - m_i a_1^i = m_i - 1, \tag{4.13}$$

$$(\hat{d}_1^i + \hat{d}_{-1}^i r_i^{-2}) - m_i \hat{b}_1^i = m_i - 1, \tag{4.14}$$

$$(c_n^i - c_{-n}^i r_i^{-2n}) - m_i a_n^i = 0, \quad n \geq 2, \tag{4.15}$$

$$(d_n^i + d_{-n}^i r_i^{-2n}) - m_i b_n^i = 0, \quad n \geq 1, \tag{4.16}$$

$$(\hat{d}_n^i + \hat{d}_{-n}^i r_i^{-2n}) - m_i \hat{b}_n^i = 0, \quad n \geq 2, \tag{4.17}$$

$$(\hat{c}_n^i - \hat{c}_{-n}^i r_i^{-2n}) - m_i \hat{a}_n^i = 0, \quad n \geq 1. \tag{4.18}$$

From these relationships we may obtain what turn out to be the important results

$$c_{-1}^i = r_i^2 \mathcal{M}_i (c_1^i + 1), \tag{4.19}$$

$$c_{-n}^i = r_i^{2n} \mathcal{M}_i c_n^i, \quad n \geq 2, \tag{4.20}$$

$$d_{-n}^i = -r_i^{2n} \mathcal{M}_i d_n^i, \quad n \geq 1, \tag{4.21}$$

$$a_1^i = \mathcal{N}_i c_1^i + \mathcal{M}_i, \tag{4.22}$$

$$b_1^i = \mathcal{N}_i d_1^i, \tag{4.23}$$

$$\hat{d}_{-1}^i = -r_i^2 \mathcal{M}_i (\hat{d}_1^i + 1), \tag{4.24}$$

$$\hat{d}_{-n}^i = -r_i^{2n} \mathcal{M}_i \hat{d}_n^i, \quad n \geq 2, \tag{4.25}$$

$$\hat{c}_{-n}^i = r_i^{2n} \mathcal{M}_i \hat{c}_n^i, \quad n \geq 1, \tag{4.26}$$

$$\hat{b}_1^i = \mathcal{N}_i \hat{d}_1^i + \mathcal{M}_i, \tag{4.27}$$

$$\hat{a}_1^i = \mathcal{N}_i \hat{c}_1^i, \tag{4.28}$$

where  $\mathcal{M}_i = (1 - m_i)/(1 + m_i)$  and  $\mathcal{N}_i = 2/(1 + m_i)$ . The further relationships required to close the system will come from the double periodicity conditions. Before we discuss this we shall show how we find the elements of  $\mathbf{H}_i$  in terms of the coefficients of the solutions for  $\mathbf{W}^i$ . From (3.7), (4.3) and (4.4) and the orthogonality of cosine and sine, we obtain

$$\mathbf{H}_i = \int_0^{2\pi} \mathbf{W}^i \cdot \mathbf{n}_i r_i d\theta, \tag{4.29}$$

$$= \int_0^{2\pi} \begin{pmatrix} W_1^i \cos \theta & W_1^i \sin \theta \\ W_2^i \cos \theta & W_2^i \sin \theta \end{pmatrix} r_i d\theta, \tag{4.30}$$

$$= |D_i| \begin{pmatrix} a_1^i & b_1^i \\ \hat{a}_1^i & \hat{b}_1^i \end{pmatrix}, \tag{4.31}$$

and by comparing this with (3.7) we see that for circular cylinders we have

$$H_{11}^i = a_1^i, \quad H_{12}^i = b_1^i, \tag{4.32}$$

$$H_{21}^i = \hat{a}_1^i, \quad H_{22}^i = \hat{b}_1^i \tag{4.33}$$

and once these coefficients have been obtained we can feed them directly into (3.25), (3.26) and (3.27) to find the leading order effective elastic moduli of the general monoclinic material.

#### 4.1. Doubly periodic functions

In order to consider a wide range of specific inclusion geometries, it is first necessary to derive doubly periodic functions which we use as building blocks for all the configurations. We must construct a doubly periodic function having period  $A$ , say, in the  $x$  direction and  $B$ , say, in the  $y$  direction, having the behaviour  $(\cos \theta, \sin \theta)/r$  as  $r \rightarrow 0$ . Thus, we will construct such a doubly periodic function of a complex variable with poles

at periodic locations in the complex plane. For the solution  $\mathbf{W}$  these poles lie outside its domain of validity  $D_0$  (i.e. *inside*  $D_i$ ) and therefore it remains analytic within  $D_0$ . Defining the complex variable  $z = x + iy = r \exp(i\theta)$  and letting  $A \in \mathbb{R}$ , we construct the function

$$\frac{1}{z} + \sum_{m=1}^{\infty} \left( \frac{1}{z - mA} + \frac{1}{z + mA} \right) = \frac{\pi}{A} \cot \left( \frac{\pi z}{A} \right) \tag{4.34}$$

which has residue unity at  $z = m, m \in \mathbb{N}$  and then on letting  $B \in \mathbb{R}$ , we define

$$\Phi^1(z; A, B) = \frac{\pi}{A} \cot \left( \frac{\pi z}{A} \right) + \frac{\pi}{A} \sum_{n=1}^{\infty} \left[ \cot \left( \frac{\pi}{A} (z - inB) \right) + \cot \left( \frac{\pi}{A} (z + inB) \right) \right] \tag{4.35}$$

which may be recast in the form

$$\Phi^1(z; A, B) = \frac{\pi}{A} \cot \left( \frac{\pi z}{A} \right) + \frac{2\pi}{A} \sin \left( \frac{2\pi z}{A} \right) \sum_{n=1}^{\infty} \left( \cosh \left( \frac{2n\pi B}{A} \right) - \cos \left( \frac{2\pi z}{A} \right) \right)^{-1}. \tag{4.36}$$

Note that the superscript 1 indicates that the potential has singular behaviour like  $1/z$  at each lattice point. The fact that the  $\pm n$  terms in (4.35) must be paired to ensure convergence means that the imaginary part of this function is *not* doubly periodic but the real part certainly *is*. Thus, the leading potential we use is

$$F^1(z; A, B) = f^1(x, y; A, B) = \Re(\Phi^1(x + iy; A, B)) \tag{4.37}$$

which is doubly periodic (with periodic  $A$  in the  $x$  direction and  $B$  in the  $y$  direction). Furthermore with the following arguments it takes on the required behaviour near the origin:

$$F^1(z; A, B) = f^1(x, y) \sim \frac{x}{x^2 + y^2} = \frac{\cos \theta}{r}, \tag{4.38}$$

$$F^1(-iz; B, A) = \hat{f}^1(x, y) \sim \frac{y}{x^2 + y^2} = \frac{\sin \theta}{r}, \tag{4.39}$$

as  $r \rightarrow 0$ . The interchange of  $A$  and  $B$  is necessary in (4.39) to retain the correct periodicity in the appropriate directions.

In order to form a multipole expansion we wish to generate a family of potentials with poles of increasing order at the lattice points  $z = mA + inB$ . One possibility would be to generalize (4.35) as

$$\left( \frac{\pi}{A} \right)^p \cot^p \left( \frac{\pi z}{A} \right) + \left( \frac{\pi}{A} \right)^p \sum_{n=1}^{\infty} \left[ \cot^p \left( \frac{\pi}{A} (z - inB) \right) + \cot^p \left( \frac{\pi}{A} (z + inB) \right) \right]$$

but this only converges for  $p$  odd and as for (4.36) is only doubly periodic in its real part. A simpler form is obtained by writing

$$\Phi^j(z; A, B) = \left( \frac{\pi}{A} \right)^j \sum_{n=-\infty}^{\infty} \frac{1}{\sin^j \left( \frac{\pi}{A} (z + inB) \right)}, \quad j = 2, 4, 6, \dots, \tag{4.40}$$

$$\Phi^j(z; A, B) = \left( \frac{\pi}{A} \right)^j \sum_{n=-\infty}^{\infty} \frac{\cos \left( \frac{\pi}{A} (z + inB) \right)}{\sin^j \left( \frac{\pi}{A} (z + inB) \right)}, \quad j = 3, 5, 7, \dots, \tag{4.41}$$

where the superscript  $j$  on  $\Phi^j$  signifies the strength of the leading order singularity and *not* a power. The absolute convergence of these infinite series means that the potentials are doubly periodic complex functions, i.e. if  $z \rightarrow z - iqB, q \in \mathbb{Z}$ , then changing  $n$  to  $n + q$  shows that the potential remains the same. Further the sums in (4.36), (4.40) and (4.41) are rapidly convergent and so are excellent for numerical purposes. It is interesting to remark that a consequence of the double periodicity of  $\Phi^j, j \geq 2$ , is that their residue must be zero.

For a general periodic cell in which there are  $N$  inclusions, centred at points  $z_i$  in the cell, we can define the functions

$$\Phi_i^j(z; A, B) = \Phi^j(z - z_i; A, B) \tag{4.42}$$

for  $1 \leq i \leq N, j \geq 2$  and where  $A$  and  $B$  are chosen to give the correct periodicity within the material. For the leading order potentials, we define

$$F_i^1(z; A, B) = \Re(\Phi^1(z - z_i; A, B)), \tag{4.43}$$

$$\hat{F}_i^1(z; B, A) = \Re(\Phi^1(z + iz_i; B, A)), \tag{4.44}$$

where the rotation of poles is required for  $\hat{F}_i^1$  since its argument in the multipole expansion to follow shortly will be  $-iz$ , as indicated by (4.39).

Considering the *full* exterior solution  $\mathbf{W} = (Y_1, Y_2)$  we can now employ the following multipole expansions for  $Y_1$  and  $Y_2$ :

$$Y_1 = \sum_{i=1}^N (\gamma_{i1}^R F_i^1(z; A, B) + \gamma_{i1}^I \hat{F}_i^1(-iz; B, A)) + \Re \left\{ \sum_{j=2}^{\infty} \sum_{i=1}^N \gamma_{ij} \Phi_i^j(z; A, B) \right\}, \tag{4.45}$$

$$Y_2 = \sum_{i=1}^N (\hat{\gamma}_{i1}^R F_i^1(z; A, B) + \hat{\gamma}_{i1}^I \hat{F}_i^1(-iz; B, A)) + \Re \left\{ \sum_{j=2}^{\infty} \sum_{i=1}^N \hat{\gamma}_{ij} \Phi_i^j(z; A, B) \right\}, \tag{4.46}$$

where  $\gamma_{i1}^R, \hat{\gamma}_{i1}^R, \gamma_{i1}^I, \hat{\gamma}_{i1}^I \in \mathbb{R}$ ,  $\gamma_{ij} = \gamma_{ij}^R + i\gamma_{ij}^I$  and  $\hat{\gamma}_{ij} = \hat{\gamma}_{ij}^R + i\hat{\gamma}_{ij}^I \in \mathbb{C}$ ,  $j \geq 2$  are constants. Note that  $\gamma_{i1}^R$  and  $\gamma_{i1}^I$  do not denote the real and imaginary parts of  $\gamma_{i1}$  unlike the notation for  $\gamma_{ij}$ ,  $j \geq 2$ ; it is merely a notational convenience.

These multipole expansions allow the system to be closed by taking their local expansions about each inclusion and using the relations (4.19)–(4.21) to obtain a linear system in  $\gamma_{ij}^R$  and  $\gamma_{ij}^I$ , as will be shown shortly. Thus, we find doubly periodic functions  $Y_1$  and  $Y_2$  which also satisfy the boundary conditions on each of the fibre/host interfaces. Since the solutions (4.45) and (4.46) must be truncated for a finite value in the  $j$  sum, say  $p$ , we note that the maximum value of  $p$  required for the solution to have converged will clearly increase as the fibre radii increase.<sup>4</sup> Each doubly periodic potential allows the boundary conditions for one of the fibres in the periodic cell to be satisfied whilst simultaneously providing double periodicity. Finally, since all coefficients in the solutions are known (to an accuracy dictated by the choice of  $p$  in the truncations of (4.45) and (4.46)), we can substitute these into (4.22), (4.23), (4.27) and (4.28) to obtain the elements of  $\mathbf{H}_i$ .

#### 4.2. Odd and even split for circular cross sections

The functions  $F_i^1(z)$  and  $\hat{F}_i^1(z)$  are odd and furthermore  $\Phi_i^j(z)$  are purely odd ( $j$  odd) (or can be made so by removal of an appropriately chosen constant) or even ( $j$  even) and therefore the odd and even parts of the multipole expansion are completely uncoupled, regardless of the geometry of the composite. For example, consider the multipole expansion of  $Y_1$ , which we truncate at  $j = p$  (odd), and separate into odd and even powers, so that

$$Y_1 = \Psi_1^O + \Psi_1^E, \tag{4.47}$$

where

$$\Psi_1^O(z) = \sum_{i=1}^N \left\{ \gamma_{i1}^R F_i^1(z; A, B) + \gamma_{i1}^I \hat{F}_i^1(-iz; B, A) + \Re \left( \sum_{j=3,5,\dots}^{\dots,p-2,p} \gamma_{ij} \Phi_i^j(z; A, B) \right) \right\}, \tag{4.48}$$

$$\Psi_1^E(z) = \sum_{i=1}^N \sum_{j=2,4,6,\dots}^{\dots,p-3,p-1} \gamma_{ij} \Phi_i^j(z; A, B) \tag{4.49}$$

are the odd and even parts of the multipole expansion, respectively.

<sup>4</sup> Note that the multipole expressions (4.45) and (4.46) remain doubly periodic if the  $j$  sum is truncated at a finite value  $p$ , say; this is equivalent to assuming that  $\gamma_{ij}$ ,  $j > p$  are sufficiently small and can be set to zero.

Now for *circular cross sections*, we only have to determine  $a_1, b_1, \hat{a}_1$  and  $\hat{b}_1$  and thus we have only to solve the *odd* system above. Further since the boundary condition does not affect the even system this system will be homogeneous and thus  $\gamma_{ij} = 0$  for *even*  $j$ .

On expanding the potential having singularity of order  $j$  (odd) and corresponding to the  $i$ th inclusion ( $1 \leq i \leq N$ ), in a Laurent (or Taylor series) expansion about the location of the  $k$ th inclusion  $z_k$ , it must have the form

$$\delta_{ik} \left( \frac{1}{(z - z_k)^j} + \sum_{m=1}^{(j-1)/2} s_{(2m-j)}^{ijk} (z - z_k)^{2m-j} \right) + \sum_{m=1}^{\infty} s_{(2m-1)}^{ijk} z^{2m-1}, \tag{4.50}$$

where the constants  $s_m^{ijk} \in \mathbb{C}$  in general and  $\delta_{ik}$  is the kronecker delta.

Thus, a local expansion of (4.48) about the  $k$ th inclusion can be written in the form

$$\Psi_{1k}^O = \Re \left( \frac{\alpha_{-p,k}}{z^p} + \frac{\alpha_{-p+2,k}}{z^{p-2}} + \dots + \alpha_{p,k} z^p \right), \tag{4.51}$$

where  $\alpha_{m,k} = \alpha_{m,k}(\gamma_{ij}) = \alpha_{m,k}^R + i\alpha_{m,k}^I \in \mathbb{C}$  depend on all  $\gamma_{ij}$ ,  $j$  odd and  $1 \leq i \leq N$ . Of course,  $\alpha_{m,k}$  for  $m < 0$  will depend only on  $\gamma_{k1}, \gamma_{k3}, \dots, \gamma_{kp}$  since the  $k$ th expansion is the only one which is a *Laurent* as opposed to a *Taylor series* expansion. Thus,

$$\begin{aligned} \Psi_{1k}^O = & \left\{ \alpha_{-p,k}^R \frac{\cos p\theta}{r^p} + \dots + \gamma_{k1}^R \frac{\cos \theta}{r} + \alpha_{1,k}^R r \cos \theta + \dots + \alpha_{p,k}^R r^p \cos p\theta \right\} \\ & + \left\{ \alpha_{-p,k}^I \frac{\sin p\theta}{r^p} + \dots + \gamma_{k1}^I \frac{\sin \theta}{r} - \alpha_{1,k}^I r \sin \theta + \dots - \alpha_{p,k}^I r^p \sin p\theta \right\}, \end{aligned} \tag{4.52}$$

where we note that the coefficient  $\alpha_{-1,k}^R$  is simply  $\gamma_{k1}^R$  and  $\alpha_{-1,k}^I$  is  $\gamma_{k1}^I$ ; this is due to the fact that the only potentials with  $1/z$  behaviour in the multipole expansion are  $F^1$  and  $\bar{F}^1$ .

We now compare (4.52) with the odd part of the solution (4.5), expanded about the location of the  $k$ th inclusion and similarly truncated, i.e.

$$\begin{aligned} Y_1^k = & \left\{ c_{-p}^k \frac{\cos p\theta}{r^p} + c_{-p+2}^k \frac{\cos(p-2)\theta}{r^{p-2}} + \dots + c_p^k r^p \cos p\theta \right\} \\ & + \left\{ -d_{-p}^k \frac{\sin p\theta}{r^p} - d_{-p+2}^k \frac{\sin(p-2)\theta}{r^{p-2}} + \dots + d_p^k r^p \sin p\theta \right\}. \end{aligned} \tag{4.53}$$

The relations (4.19), (4.20) and (4.21), for the  $k$ th inclusion, i.e.

$$c_{-1}^k = r_1^2 \mathcal{M}_k (c_1^k + 1), \tag{4.54}$$

$$c_{(-2n-1)}^k = r_1^{2(2n+1)} \mathcal{M}_k c_{(2n+1)}^k, \quad 1 \leq n \leq (p-1)/2, \tag{4.55}$$

$$d_{(-2n-1)}^k = -r_1^{2(2n+1)} \mathcal{M}_k d_{(2n+1)}^k, \quad 0 \leq n \leq (p-1)/2, \tag{4.56}$$

then provide  $p + 1$  linear equations in terms of the  $N(p + 1)$  unknowns  $\gamma_{ij}^R$  and  $\gamma_{ij}^I$ , for  $j = 1, 3, \dots, p$  and  $i = 1, 2, \dots, N$ . Thus if we carry out the above for each of the remaining  $N - 1$  inclusions in the periodic cell, we obtain the full system of  $N(p + 1)$  linear equations for the  $N(p + 1)$  unknowns. Having solved this system, each coefficient  $c_n^i$  is then known and in particular  $a_1^i$  and  $b_1^i$  may be calculated by virtue of (4.22) and (4.23):

$$a_1^i = \mathcal{N}_i c_1^i + \mathcal{M}_i, \tag{4.57}$$

$$b_1^i = \mathcal{N}_i d_1^i. \tag{4.58}$$

The calculations for  $Y_2$  proceed analogously, giving us values for  $\hat{a}_1^i$  and  $\hat{b}_1^i$  and thus the effective properties from (3.25) to (3.27) together with (4.32) and (4.33). In general the coefficients  $s_m^{ijk}$  in the series expansions (4.50) are complex. If they were purely real, it would mean that  $\alpha_{m,k}^R$  depend only on  $\gamma_{ij}^R$  and  $\alpha_{m,k}^I$  depend only on  $\gamma_{ij}^I$ . This decoupling then means that (4.56) becomes a homogeneous linear system in  $\gamma_{ij}^I$  and thus  $\gamma_{ij}^I = 0$ . Furthermore this means that  $d_1^i = 0$  and thus from (4.58),  $b_1^i = 0$ . Similarly we may show that if the

corresponding constants in the expansions for  $Y_2$  are real,  $\hat{a}_1^i = 0$ . Thus from (3.27) with (4.32) and (4.33),  $m_{xy}^* = 0$ . Constants in the local expansions of potentials corresponding to orthotropic media are always real and thus the theory is consistent as we shall see in the next section.

To proceed we shall specify certain geometries and show how the above may be implemented in these cases. Note that we only had to solve the odd system above because the fibres had circular cross section. For more general cross sections, the odd and even systems are still uncoupled but since the effective properties will depend on more coefficients than simply  $a_1^i, b_1^i, \hat{a}_1^i$  and  $\hat{b}_1^i$ , we are required to solve both systems to find the effective properties (see Section 6).

### 5. Specific geometries

#### 5.1. Rectangular lattice – orthotropic

Consider a material like the one in Fig. 1(c). The periodic cell has one fibre inside it ( $N = 1$ ) located at  $z_1 = 0$  with radius  $r_1$ . Take the horizontal period to be  $A_1 = A$  and the vertical period to be  $B_1 = 1$ . Therefore we require only one set of potentials in the multipole expansions (4.45) and (4.46) which are given by

$$Y_1 = \gamma_1^R F^1(z; A, 1) + \gamma_1^I \hat{F}^1(-iz; 1, A) + \Re \left\{ \sum_{j=1}^{\infty} \gamma_j \Phi^j(z; A, 1) \right\}, \tag{5.1}$$

$$Y_2 = \hat{\gamma}_1^R F^1(z; A, 1) + \hat{\gamma}_1^I \hat{F}^1(-iz; 1, A) + \Re \left\{ \sum_{j=1}^{\infty} \hat{\gamma}_j \Phi^j(z; A, 1) \right\}. \tag{5.2}$$

Note that since there is only one inclusion in the periodic cell we have dropped the subscript  $i$  on the coefficients  $\gamma_{ij}, \hat{\gamma}_{ij}$  and on the potentials. We recall from the previous section that  $\gamma_j = \hat{\gamma}_j = 0$  for  $j$  even. Since there is only one fibre in the periodic cell, the expansions of the potentials (4.50) about the origin have the form

$$\frac{1}{z^j} + \sum_{k=1}^{\infty} s_{(2k-j)}^j z^{2k-j}. \tag{5.3}$$

In these expansions,  $s_{(2k-j)}^j$  are real and thus as discussed above this predicts that  $m_{xy}^* = 0$ , as it should do in this case. For  $Y_1$  ( $Y_2$ ) we have a system of  $(p + 1)/2$  linear equations to solve for  $\gamma_j^R$  ( $\gamma_j^I$ ) which, once solved provides us with the effective properties  $m_x^*$  and  $m_y^*$  from (3.25) and (3.26).

We shall now show some results for various types of these orthotropic materials, with specific cylinder radii  $r_1$  and elastic moduli  $m_1 = \mu_1/\mu_0$ . All the results have been computed in Mathematica.

##### 5.1.1. Square lattice

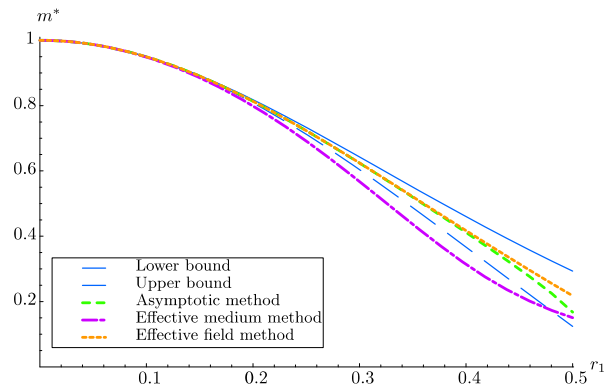
By taking  $A = 1$  we obtain a square lattice which corresponds to tetragonal symmetry and six elastic constants. For this material we should find that  $m_x^* = m_y^* = m^*$  (meaning that the material is transversely isotropic for SH waves) and indeed computations show this to be the case here. Table 1 shows how solutions converge for different fibre radii with  $m_1 = 10$ ; dashes (–) indicate that the solution has converged to the accuracy shown (six significant figures). For radii up to  $r_1 = 0.15$  convergence is excellent with only 1 term in the multipole expansion required for full convergence. Furthermore when fibres are close to touching ( $r_1 = 0.495$ ), even though convergence to six decimal places requires  $p = 49$ , this calculation only takes 0.85 seconds in Mathematica. In actual fact  $p = 49$  means that we take only 25 terms in the multipole expansion. This appears to compare very favourably with other asymptotic methods such as McPhedran et al. [14] where in the case of determining the effective conductivity of a square array of closely touching cylinders the accuracy of the multipole expansion appears to be affected by the physical properties of the fibres. Even after restricting these properties it appears that many terms ( $\geq 100$ ) are required in their multipole expansions. Our method outlined above has no such restrictions.

In Fig. 3 we compare our results for the parameter  $m_1 = 0.1$  with other homogenization methods. We see that our result lies within the Hashin bounds [6]. We plot the effective medium result noting that it provides

Table 1

Table showing convergence of the multipole method for a square array with  $m_1 = 10$  and various radii

Square array, $m_1 = 10$					
$p$	$r_1 = 0.05$	$r_1 = 0.1$	$r_1 = 0.15$	$r_1 = 0.2$	$r_1 = 0.25$
1	1.01294	1.05276	1.12277	1.2292	1.3828
3	–	–	–	1.22921	1.38293
5	–	–	–	–	–
$p$	$r_1 = 0.3$	$r_1 = 0.35$	$r_1 = 0.4$	$r_1 = 0.45$	$r_1 = 0.495$
1	1.60192	1.91917	2.3971	3.17105	4.40264
3	1.60294	1.92523	2.42882	3.3343	5.22256
5	–	1.92524	2.42895	3.33885	5.36013
11	–	–	2.42903	3.34072	5.45375
19	–	–	–	3.34049	5.33262
49	–	–	–	–	5.45806
51	–	–	–	–	–

Fig. 3. Comparing the prediction of the effective longitudinal shear modulus (plotted against radius of fibre cross section) of a tetragonal material by various methods for the value  $m_1 = 0.1$ .

a useful approximation for small volume fractions but for larger volume fractions where the geometry becomes more significant the approximations inherent in the method lead to significant errors, drifting outside the variational bounds. We also plot the effective field and  $T$ -matrix methods which provide a good approximation to the exact result. Our results also concur with those given in Fig. 4 of Sabina et al. [23] when we use the relevant parameter sets. This illustrates that the quasi-static limit is equivalent to the MAH for statics, as of course it should be. Finally in Table 2 we compare our results for the square lattice with those obtained via the equivalent inclusion method by Jiang et al. [10] and the computational results of Chen [3] and Adam and Doner [1].

### 5.1.2. Rectangular lattice

We shall illustrate the case of a rectangular lattice by taking  $A = 2$ ,  $B = 1$ . The material is then strictly orthotropic. We implement the method described above and obtain the results shown in Figs. 4 and 5. Note in particular that for this case regardless of the value of the parameter  $m_1$ , the shear modulus corresponding to shearing in a plane perpendicular to the  $y$  axis  $m_y^*$  is *always* greater than  $m_x^*$ . This is because we can think of the composite as having *layers* of low shear modulus material (corresponding either to columns of low shear modulus fibre ( $m_1 < 1$ ) or low shear modulus host ( $m_1 > 1$ )) perpendicular to the  $x$  axis. This weakens the response to shearing in planes perpendicular to the  $x$  axis; hence the lower effective shear modulus  $m_x^*$ . We see a further

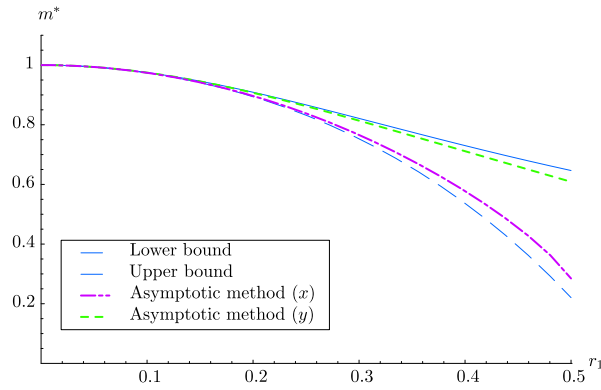


Fig. 4. The results of the method of asymptotic homogenization for the rectangular lattice structure, with  $m_1 = 0.1$ .

Table 2  
Table comparing the results of different methods for  $m_x^* = m_y^*$  at various volume fractions

$\phi$	$r_1$	$m_1$	MAH	Jiang et al.	Chen	Adam/Doner
0.4	0.356825	6	1.80451	1.80451	1.805	1.796
		20	2.14586	2.14586	2.147	2.137
		120	2.31344	2.31343	2.314	2.305
		400	2.33957	2.33957	2.340	–
0.55	0.418414	6	2.3256	2.32562	2.326	2.304
		20	3.07708	3.07712	3.184	3.044
		120	3.50657	3.50663	3.555	3.469
		400	3.57782	3.57789	3.578	–
0.7	0.472035	6	3.17309	3.17311	3.176	3.163
		20	5.21285	5.21367	5.222	5.187
		120	6.92746	6.92945	6.945	6.878
		400	7.2714	7.27364	7.291	–
0.75	0.4886025	6	3.61827	3.61966	3.620	3.646
		20	7.00108	7.00409	7.006	7.005
		120	11.1536	11.1640	11.170	11.035
		400	12.2137	12.2264	12.523	–

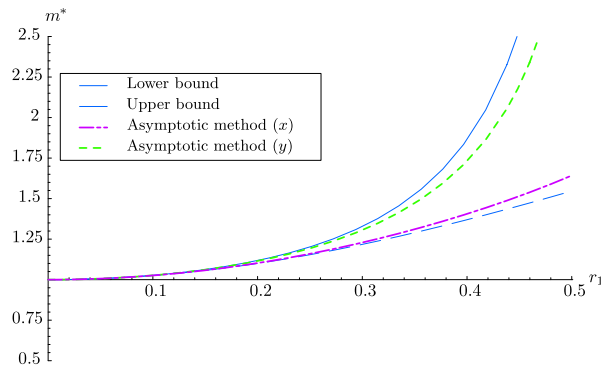


Fig. 5. The results of the method of asymptotic homogenization for the rectangular lattice structure, with  $m_1 = 10$ .

example of this type of behaviour in Section 5.3 where we consider a more complicated orthotropic material. Note that the results sit inside the corresponding Hashin bounds for this material.

5.2. Hexagonal lattice – transversely isotropic

Consider a material consisting of fibres arranged on a hexagonal lattice, as shown in Fig. 1(e). This material is transversely isotropic and computations confirm that  $m_x^* = m_y^* = m^*$ . In order to construct this hexagonal symmetry it is necessary to add together two families of potentials. Let  $z_2 = (1 + i\sqrt{3})/2$  and define

$$G^1(z) = \Re\left(\Phi^1(z; A = 1, B = \sqrt{3}) + \Phi^1(z - z_2; A = 1, B = \sqrt{3})\right), \tag{5.4}$$

$$\hat{G}^1(z) = \Re\left(\Phi^1(z; A = 1, B = \sqrt{3}) + \Phi^1(z + iz_2; A = \sqrt{3}, B = 1)\right), \tag{5.5}$$

$$\Psi^j(z) = \Phi^j(z; A = 1, B = \sqrt{3}) + \Phi^j(z - z_2; A = 1, B = \sqrt{3}), \quad j \geq 3, \tag{5.6}$$

and we use these functions in our multipole expansions:

$$Y_1 = \gamma_1^R G_i^1(z) + \gamma_1^I \hat{G}_i^1(-iz) + \Re\left\{\sum_{j=1}^{\infty} \gamma_j \Phi^j(z)\right\}, \tag{5.7}$$

$$Y_2 = \hat{\gamma}_1^R G_i^1(z) + \hat{\gamma}_1^I \hat{G}_i^1(-iz) + \Re\left\{\sum_{j=1}^{\infty} \hat{\gamma}_j \Phi^j(z)\right\}. \tag{5.8}$$

We plot the results for a hexagonal lattice in Fig. 6 using  $m_1 = 10$ . In this instance the  $T$ -matrix result provided by Varadan et al. [26] should provide a reasonable comparison with the MAH result since it was derived under the assumption that the random material was transversely isotropic. This result is actually a special limit of the Hashin bounds where the area not occupied by composite cylinders tends to zero and the bounds coincide [6]. In particular, if we accept the assumptions of the  $T$ -matrix method in this case, this comparison will be a good indication of how different the response of random and periodic transversely isotropic materials are, when excited by SH waves. Since the effective field method can be shown to be equivalent to the  $T$ -matrix scheme this provides a good approximation in this case, unlike the effective medium method which gives only a reasonable approximation for small volume fractions.

5.3. Other orthotropic materials

Consider an orthotropic material with periodic cell as shown in Fig. 7. This cell consists of two fibres ( $N = 2$ ) with radii and shear moduli parameters,  $r_1, m_1$  and  $r_2, m_2$ , respectively. To construct the multipole expansion for  $Y_1$  we use the form (5.1) with  $N = 2$  and two sets of the potentials (4.43), (4.44) and (4.42), one for each of the locations  $z_1 = 0$  and  $z_2 = 1$ . The effective moduli are thus given by

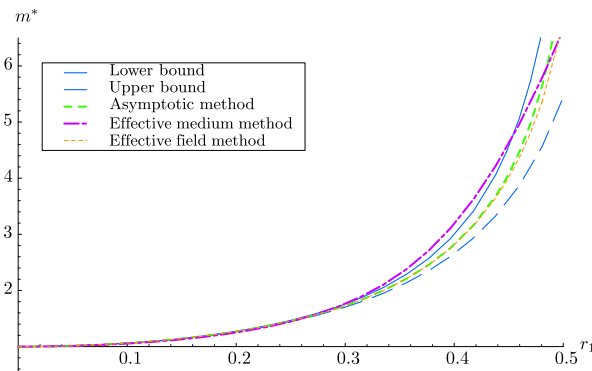


Fig. 6. Comparing the method of asymptotic homogenization with various other methods for the value  $m_1 = 10$  for hexagonal symmetry.

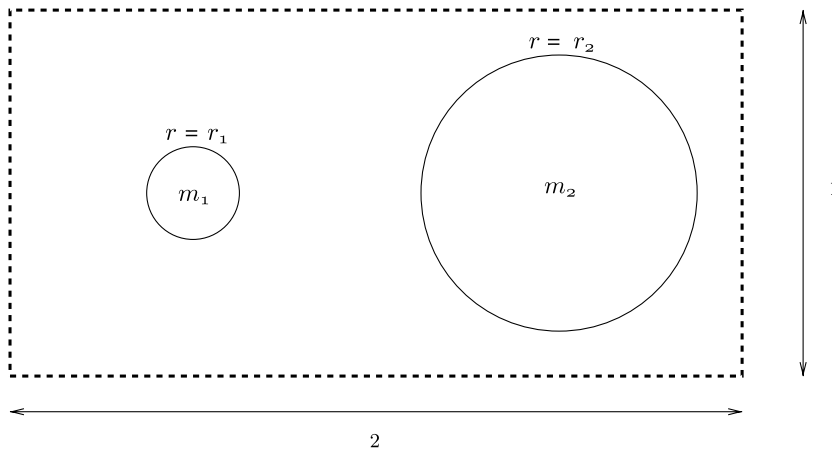


Fig. 7. A typical periodic cell of the orthotropic material discussed in Section 5.3. The periodic cell consists of two circular fibres each of different radii and distinct shear moduli.

$$\rho_* = 1 + \phi_1(d_1 - 1) + \phi_2(d_2 - 1), \tag{5.9}$$

$$m_x^* = 1 + \phi_1(m_1 - 1)(1 + a_1^1) + \phi_2(m_2 - 1)(1 + a_1^2), \tag{5.10}$$

$$m_y^* = 1 + \phi_1(m_1 - 1)(1 + \hat{b}_1^1) + \phi_2(m_2 - 1)(1 + \hat{b}_1^2), \tag{5.11}$$

where it is stressed that the superscripts distinguish between fibres and are *not* powers. As is evident, this procedure can easily be extended to any number of fibres included in the periodic cell, enabling complicated structures to be modelled. It is easy to see the application of such a material in industry – it is possible to obtain effective shear moduli with this type of structure which may not be obtainable with a single type fibre reinforced material.

For orthotropic materials on a rectangular lattice as described in Section 5.1, it is possible to show that even for high contrast materials ( $m_1 \gg 1$  or  $m_1 \ll 1$ ) the effective shear moduli in the  $x$  and  $y$  directions are still relatively close. In contrast let us consider the *two-fibre periodic cell* material described above. Let each fibre have the same radius  $r_1$  and consider varying their shear moduli.

Set  $m_1 = 100$  and  $m_2 = 0.01$  (or  $m_1 = 0.01, m_2 = 100$ , since this is equivalent). This corresponds to alternating columns of very high and very low shear modulus fibres (compared with the host material). We would thus expect the response to shearing perpendicular to the  $x$  axis to be weakened for there are now layers of material with low shear modulus perpendicular to this axis. Alternatively we expect the resistance to shearing in a direction perpendicular to the  $y$  axis to be *increased* since each plane perpendicular to this direction contains high shear modulus fibres.

We plot some results in Table 3 for various radii of fibres, as usual analysing convergence. When the fibres are almost touching at  $r = 0.495$ , the shear modulus in the  $x$  direction is reduced to approximately one eighth of that of the host shear modulus whilst that in the  $y$  direction is increased to almost eight times that of the host shear modulus. To show the contrast between the shear moduli in the two directions we plot the ratio  $m_y^*/m_x^*$  in Fig. 8. In particular note that for materials with larger radii fibres, the contrast in shear modulus can be very large.

#### 5.4. Fully monoclinic materials

As we discussed above, if we break lines of symmetry in the periodic cell the material becomes monoclinic. To the authors knowledge no results have been published in the literature regarding the effective elastic moduli of monoclinic fibre reinforced composites. Let us construct a monoclinic material by considering a periodic cell containing four fibres, all centred on a square lattice except for one which has been perturbed off its lattice point by a radial distance  $|\xi|$  (see Fig. 1(a)). Provided  $\xi \in \mathbb{C}$  and is not purely real

Table 3

Table showing convergence of the effective shear moduli for the “two-fibre” periodic cell material described above

Two-fibre periodic cell, $m_1 = 100, m_2 = 0.01$						
$p$	$r = 0.1$	$r = 0.2$	$r = 0.3$	$r = 0.4$	$r = 0.45$	$r = 0.495$
$m_x^*$						
1	0.997927	0.967339	0.84494	0.580245	0.403033	0.232324
3	–	0.967337	0.844736	0.574983	0.382846	0.167835
5	–	–	0.844735	0.57477	0.380429	0.144596
7	–	–	–	0.574762	0.380103	0.134266
9	–	–	–	0.574761	0.380072	0.130021
13	–	–	–	–	0.380064	0.12664
31	–	–	–	–	–	0.125463
33	–	–	–	–	–	–
$m_y^*$						
1	1.00208	1.03376	1.18352	1.72341	2.48118	4.30433
3	–	1.03377	1.1838	1.73918	2.61202	5.95823
5	–	–	–	1.73983	2.62861	6.91583
7	–	–	–	1.73985	2.63087	7.44791
11	–	–	–	–	2.63113	7.82931
13	–	–	–	–	–	7.8964
41	–	–	–	–	–	7.97196
43	–	–	–	–	–	–

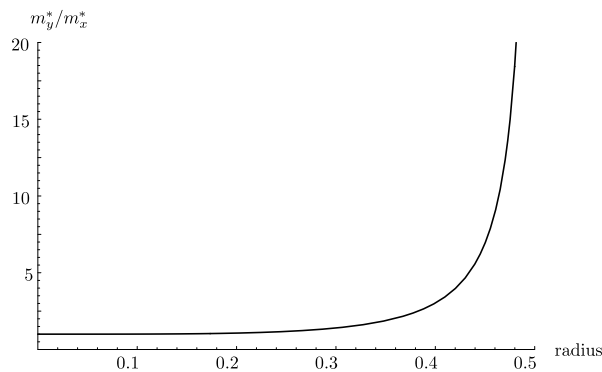


Fig. 8. The contrast between shear moduli in the  $x$  and  $y$  directions for the two fibre periodic cell material, where  $m_1 = 0.01, m_2 = 100$ . Note that for high radii, very large contrasts are possible. It is not possible to obtain such high contrast effective moduli in fibre reinforced materials with only one fibre type.

or imaginary, this material is strictly monoclinic. We construct the multipole expansion for  $Y_1$  from four sets of potentials, one for each of the positions  $z_1 = \zeta, z_2 = 1, z_3 = i$  and  $z_4 = 1 + i$ . The shift of the pole off the origin to  $\zeta \in \mathbb{C}$  means that the constants  $s_m^{ijk}$  in the series expansions (4.50) of the potentials will now in general be complex and as described earlier this means that the linear system is now fully coupled, leading to non-zero values for  $\hat{a}_1$  and  $b_1$  and thus a non-zero  $m_{xy}^*$ . The non-dimensional effective moduli are thus given by (3.25)–(3.27) with  $N = 4$ . Results for the specific perturbation  $\zeta = 0.1 - 0.2i$  are shown in Table 4. We can compare these results with those shown in Fig. 1, corresponding to fibres on a square lattice, also with  $m = 10$ . Clearly as  $\zeta \rightarrow 0$  the results for the monoclinic material considered here should converge to the square lattice result and it is easily shown that they do. It is clear that the monoclinicity only becomes apparent for larger volume fractions when the symmetry breaking becomes more significant. When  $m < 1$  the monoclinicity is even weaker so that rigid fibres have a greater effect on the anisotropy (monoclinicity) of the composite.

Table 4

Table showing convergence of the effective moduli for the monoclinic material described above with the specific perturbation  $\zeta = 0.1 - 0.2i$

Monoclinic material, $m_1 = m_2 = m_3 = m_4 = 10$ , $r_1 = r_2 = r_3 = r_4 = r$ , $\zeta = 0.1 - 0.2i$					
p	$r = 0.1$	$r = 0.2$	$r = 0.3$	$r = 0.35$	$r = 0.4$
$m_x^*$					
1	1.05271	1.22811	1.59452	1.90211	2.35833
3	–	1.22813	1.59583	1.90921	2.39264
5	–	–	1.59585	1.90934	2.39362
7	–	–	–	1.90935	2.39374
11	–	–	–	–	2.39379
13	–	–	–	–	–
$m_y^*$					
1	1.05282	1.2303	1.60966	1.93743	2.44
3	–	1.23033	1.61106	1.94546	2.48378
5	–	–	1.61109	1.94582	2.49028
7	–	–	–	1.94587	2.49295
19	–	–	–	–	2.49461
21	–	–	–	–	–
$m_{xy}^*$					
1	0	0	0	0	0
5	$5.9867 \times 10^{-11}$	$2.97788 \times 10^{-7}$	$4.87101 \times 10^{-5}$	$3.90392 \times 10^{-4}$	0.00329804
7	–	$2.97831 \times 10^{-7}$	$4.88903 \times 10^{-5}$	$3.9624 \times 10^{-4}$	0.00361183
13	–	–	$4.89051 \times 10^{-5}$	$3.97398 \times 10^{-4}$	0.00386808
15	–	–	–	$3.97399 \times 10^{-4}$	0.00387911
29	–	–	–	–	0.00388908
31	–	–	–	–	–

5.5. Rigid fibres and cavities

Two important cases to consider for fibre reinforced media are those extreme cases of rigid fibres (corresponding to the limit as  $m_1 \rightarrow \infty$ ) and cylindrical cavities (corresponding to the limit as  $m_1 \rightarrow 0$ ). These examples are illustrated for a square lattice in Figs. 9 and 10, respectively, where we note that the results remain inside the variational bounds. The effective medium method fails to stay inside these bounds for anything other than dilute volume fractions and in particular it predicts that  $m^* = 0$  for  $0.4 \leq r \leq 0.5$ , in the case of cavities. Note that the asymptotic method exhibits excellent converge even when the fibres or cavities are close

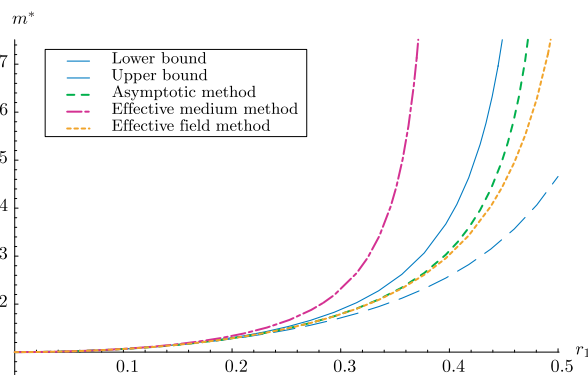


Fig. 9. Comparing the prediction of the effective longitudinal shear modulus (plotted against radius of fibre cross section) of a tetragonal material by various methods for rigid fibres (the limit as  $m_1 \rightarrow \infty$ ).

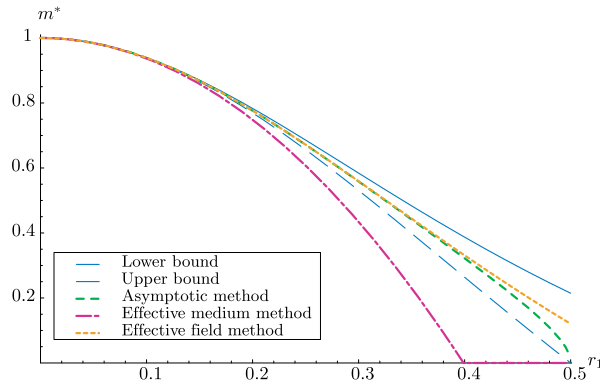


Fig. 10. Comparing the prediction of the effective longitudinal shear modulus (plotted against radius of fibre cross section) of a tetragonal material by various methods for cylindrical cavities (the limit as  $m_1 \rightarrow 0$ ).

to touching. The  $T$ -matrix/effective field methods provide good approximations over large ranges of volume fractions.

**6. Fibres of general cross section**

Until now the method has only been demonstrated on materials having fibres of circular cross section. As a result of this we have been able to solve the  $O(\epsilon)$  problem exactly via multipole expansions and the problem simplified since the boundary conditions implied that consideration of only the *odd* part of the system was necessary. The method is, however, not restricted to specific cross-sectional geometries as we shall now show. Very few results are available in the literature for materials having non-circular fibres. Jiang et al. [9] considered elliptical fibres via a generalized self-consistent method and hence obtained results for a random distribution and orientation of elliptical fibres in the  $xy$  plane. In the context of transport theory, Nicorovici and McPhedran [17] used Rayleigh’s method and an elliptical coordinate system in order to evaluate the effective dielectric constant of a material with fibres of elliptical cross section. Here we wish to employ a general scheme suitable for arbitrary fibres with smooth boundaries.

Let us consider a fibre of general cross section whose interface with the host medium in the  $xy$  plane is given in terms of polar coordinates by

$$r = f(\theta), \tag{6.1}$$

where  $f(\theta)$  is continuous and at least once differentiable. Thus the normal to this interface is given by

$$\mathbf{n} = \frac{1}{\sqrt{f^2 + f_\theta^2}} (f \cos \theta + f_\theta \sin \theta, f \sin \theta - f_\theta \cos \theta), \tag{6.2}$$

where  $f_\theta = \partial f / \partial \theta$  and

$$\mathbf{n} \cdot \nabla = \frac{1}{\sqrt{f^2 + f_\theta^2}} \left( f \frac{\partial}{\partial r} - \frac{f_\theta}{f} \frac{\partial}{\partial \theta} \right) \tag{6.3}$$

on the boundary. We restrict attention here to fibres positioned on a square lattice, posing multipole expansions as in (5.1) and (5.2) using the potentials  $F^1(z; 1, 1)$ ,  $\hat{F}^1(z; 1, 1)$  and  $\Phi^j(z; 1, 1)$ . We express the solutions in local polar coordinates in exactly the same way as in (4.3)–(4.6) and apply the boundary conditions on  $r = f(\theta)$ . Truncating the solutions as before, the boundary conditions for  $W_1$  and  $Y_1$  are then

$$a_0 - c_0 + \sum_{n=1}^p ((a_n - c_n)f^n \cos n\theta + (b_n - d_n)f^n \sin n\theta - c_{-n}f^{-n} \cos n\theta + d_{-n}f^{-n} \sin n\theta) = 0, \tag{6.4}$$

and

$$\begin{aligned} &\sum_{n=1}^p n[(c_n - m_i a_n) \cos n\theta + (d_n - m_i b_n) \sin n\theta] f^n - (c_{-n} \cos n\theta + d_{-n} f^{-n} \sin n\theta) f^{-n} \\ &\quad + f_\theta [(c_n - m_i a_n) \sin n\theta - (d_n - m_i b_n) \cos n\theta] f^{n-1} - (c_{-n} \sin n\theta + d_{-n} \cos n\theta) f^{-n-1} \\ &= (m_i - 1)(f \cos \theta + f_\theta \sin \theta). \end{aligned} \tag{6.5}$$

There are  $2p + 1$  unknowns  $a_m$  and  $b_m$  present in (6.4) and (6.5). Therefore in total, given that we know the relationships  $c_m = c_m(\gamma_1^R, \gamma_2^R, \dots, \gamma_p^R, \gamma_1^I, \gamma_2^I, \dots, \gamma_p^I)$  and  $d_m = d_m(\gamma_1^R, \gamma_2^R, \dots, \gamma_p^R, \gamma_1^I, \gamma_2^I, \dots, \gamma_p^I)$  from the matching between the multipole expansion  $Y_1$  and the local external solution  $Y_1^l$ , we have a total of  $4p + 1$  unknowns in (6.4) and (6.5).

In order to form a system of  $4p + 1$  equations in these unknowns, multiply (6.4) by  $\cos q\theta$ , for  $0 \leq q \leq p$  and integrate over the range  $\theta \in [0, 2\pi]$ . Next multiply (6.4) by  $\sin q\theta$ , for  $1 \leq q \leq p$  and integrate over the range

Table 5

Table showing convergence of the effective shear moduli for a fibre reinforced material where the fibres are of elliptical cross section with  $b = 0.1$  and  $m_1 = 10$

Elliptical cross section, $m_1 = 10, b = 0.1$				
$p$	$a = 0.1$	$a = 0.2$	$a = 0.3$	$a = 0.4$
$m_x^*$				
1	1.05276	1.19325	1.40698	1.65036
5	–	1.19716	1.429	1.7045
9	–	1.19737	1.43316	1.72246
13	–	1.19739	1.43438	1.73104
17	–	–	1.43479	1.73566
21	–	–	–	1.73831
23	–	–	–	–
$m_y^*$				
1	1.05276	1.13649	1.2905	1.48043
5	–	1.1362	1.28948	1.47869
9	–	–	1.28944	1.47855
21	–	–	–	1.47841
23	–	–	–	–

Table 6

Table showing convergence of the effective shear moduli for a fibre reinforced material where the fibres are of elliptical cross section with  $b = 0.25$  and  $m_1 = 10$

Elliptical cross section, $m_1 = 10, b = 0.25$				
$p$	$a = 0.1$	$a = 0.2$	$a = 0.3$	$a = 0.4$
$m_x^*$				
1	1.20748	1.28066	1.53742	1.9916
5	1.20684	1.28006	1.54554	2.09779
7	1.20683	1.28005	1.54555	2.10218
17	–	–	–	2.10376
19	–	–	–	–
$m_y^*$				
1	1.29471	1.34149	1.45017	1.66237
5	1.30575	1.34453	1.44767	1.65237
7	1.30667	1.34454	1.44766	1.65194
11	1.30722	–	–	1.65181
15	1.30734	–	–	1.6518
17	–	–	–	–

$\theta \in [0, 2\pi]$ . These operations generate  $2p + 1$  equations. Finally repeat this for (6.5) except that when multiplying by  $\cos q\theta$ ,  $q$  is limited to the range  $1 \leq q \leq p$ . This generates an extra  $2p$  equations. We thus have a linear system of  $4p + 1$  equations for  $4p + 1$  unknowns. For the sake of implementation we can split the odd and even parts of the multipole expansions as described in the previous section to obtain two smaller uncoupled systems, one of  $2p + 1$  equations and one of  $2p$  equations. The coefficients for  $Y_2$  and  $W_2$  are found analogously.

We can therefore find the quasi-static effective moduli by calculating the elements of the tensor  $\mathbf{H}_i$  defined by (3.7), where

$$H_{j1} = \frac{1}{D_i} \int_0^{2\pi} \frac{f(f \cos \theta + f_\theta \sin \theta)}{\sqrt{f^2 + f_\theta^2}} W_j^i \Big|_{r=f(\theta)} d\theta, \quad (6.6)$$

$$H_{j2} = \frac{1}{D_i} \int_0^{2\pi} \frac{f(f \sin \theta - f_\theta \cos \theta)}{\sqrt{f^2 + f_\theta^2}} W_j^i \Big|_{r=f(\theta)} d\theta \quad (6.7)$$

and  $W_j^i$  ( $j = 1, 2$ ) are the interior solutions given by (4.3) and (4.4). In the case of circular cross sections these integrals consisted of only one term due to the presence of only  $\cos \theta$  and  $\sin \theta$  in the boundary condition. For these more general cross sections the integrals result in an infinite series which we must truncate.

As an example, let us take elliptical cross sections so that

$$f(\theta) = \frac{ab}{\sqrt{a^2 \sin^2 \theta + b^2 \cos^2 \theta}} \quad (6.8)$$

and the ellipse intersects the  $x$  axis at  $x = \pm a$  and the  $y$  axis at  $y = \pm b$ . Tables 5 and 6 exhibit the convergence of the method above in the case of elliptical cross section. We consider  $m_1 = 10$  (i.e. the shear modulus of the inclusion material is significantly higher than that of the host material), and vary  $a$  for fixed  $b$ . Table 5 shows results for  $b = 0.1$  and we note that  $a = 0.1$  corresponding to circular inclusions recovers the case of tetragonal symmetry for SH waves as it should do. For higher  $a$  the ellipse becomes elongated in the  $x$  direction, creating layers of low shear modulus host material perpendicular to the  $y$  axis. We therefore expect  $m_x^* > m_y^*$  for fixed  $a > b$  and this is verified in Table 5. Similar results may be observed in Table 6 where  $b = 0.25$  where it should be noted that  $m_x^* < m_y^*$  for  $a < 0.25 = b$  and  $m_x^* > m_y^*$  for  $a > 0.25 = b$ .

## 7. Conclusions

Using the well-known approach of asymptotic homogenization we have derived an effective (homogenized) anisotropic wave Eq. (3.9) governing the propagation of SH waves within a fully monoclinic fibre reinforced material in the low frequency (quasi-static) case,  $qk_0 \ll 1$ . Thus new expressions for the effective elastic constants of the material have been derived in simple closed forms (3.24)–(3.27). The unknowns in these expressions may be found by employing multipole expansions in families of doubly periodic functions. As was shown in Section 5 these expansions are extremely convergent and results can be computed in seconds. Furthermore the routines used to calculate the results are robust, enabling many terms of the multipole expansion to be computed when necessary. The scheme also works well (without modification) when fibres are close to touching. It is therefore preferable to Rayleigh's method which requires special treatment in this limit.

The method allows complicated structures to be modelled as was shown in Section 5 where we exhibited new results for materials having full monoclinicity. Furthermore there is no restriction to fibres of circular cross section as was shown in Section 6 where we extended the method to non-circular shapes, providing new results for the case of elliptical cross sections. Other cross-sectional shapes, including non-smooth boundaries such as those with polygonal cross section, can and will be analysed in future articles. It will also be interesting to analyse other distributions of inclusions inside the periodic cell other than those discussed above.

We note that we have only achieved the leading order (quasi-static) behaviour of the effective moduli and that for dynamic effects to become apparent we must find the higher order terms which will be an algebraically

arduous task. However, the closed form expressions developed here for static properties are preferable to the existing expressions given by Meguid and Kalamkarov [15] and Sabina et al. [23] due primarily to their simplicity, rapid convergence even for fibres close to touching and their easily extendable nature to materials having complex structure. In particular note that we have not appealed directly to the theory of Weierstrassian elliptic functions in order to find the effective properties. Furthermore we have derived the results from the *dynamic* problem where the small parameter  $\epsilon$  is a *physical* quantity relating the lengthscale of the micro and macro lengthscales. This is preferable to the static approach of Meguid and Kalamkarov [15] and Sabina et al. [23] where the corresponding small parameter is somewhat fictitious and higher order terms do not have any physical significance. In contrast, the higher order terms here relate to dispersion, characterizing the (low frequency) dynamic response of the material. This will be discussed in future articles.

The method presented here may be straightforwardly extended to other elastic wave propagation problems in order to find the remaining 10 effective moduli characterizing a monoclinic material. This will also be reported on in future articles.

### Acknowledgements

Parnell was supported by an EPSRC CASE award in collaboration with Thales Underwater Systems Ltd. when this work was carried out. Abrahams gratefully received a Royal Society Leverhulme Trust Senior Research Fellowship during the course of this work. The authors thank Dr. Andrew Hazel for helpful comments on the material in Section 6.

### References

- [1] D.F. Adam, D.R. Doner, Longitudinal shear loading of a unidirectional composite, *J. Compos. Mater.* 1 (1) (1967) 4–17.
- [2] N. Bakhvalov, G. Panasenko, *Homogenization: Averaging Processes in Periodic Media*, Kluwer, Dordrecht, 1989.
- [3] C.H. Chen, Fiber reinforced composites under longitudinal shear loading, *ASME J. Appl. Mech.* 37 (1970) 198–201.
- [4] G.A. Francfort, Homogenization and linear thermoelasticity, *SIAM J. Math. Anal.* 14 (1983) 696–708.
- [5] K.F. Graff, *Wave Motion in Elastic Solids*, Dover, New York, 1991.
- [6] Z. Hashin, B.W. Rosen, The elastic moduli of fiber-reinforced materials, *J. Appl. Mech.* 31 (1964) 223–232.
- [7] Z. Hashin, S. Shtrikman, A variational approach to the theory of the elastic behaviour of multiphase materials, *J. Mech. Phys. Solids* 11 (1963) 127–140.
- [8] T. Iwakuma, S. Nemat-Nasser, Composites with periodic microstructure, *Comput. Struct.* 16 (1983) 13–19.
- [9] C.P. Jiang, Z.H. Tong, Y.K. Cheung, A generalized self-consistent method accounting for fiber section shape, *Int. J. Sol. Struct.* 40 (2003) 2589–2609.
- [10] C.P. Jiang, Y.L. Xu, Y.K. Cheung, S.H. Lo, A rigorous method for doubly periodic cylindrical inclusions under longitudinal shear and its application, *Mech. Mater.* 36 (2004) 225–237.
- [11] S.K. Kanaun, V.M. Levin, Self-consistent methods in the problem of axial elastic shear wave propagation through fiber composites, *Arch. Appl. Mech.* 73 (2003) 105–130.
- [12] A.E.H. Love, *A Treatise on the Mathematical Theory of Elasticity*, Dover, New York, 1944.
- [13] R.C. McPhedran, A.B. Movchan, The Rayleigh multipole method for linear elasticity, *J. Mech. Phys. Solids* 42 (5) (1994) 711–727.
- [14] R.C. McPhedran, L. Poladian, G.W. Milton, Asymptotic studies of closely spaced, highly conducting cylinders, *Proc. R. Soc. Lond. A* 415 (1988) 185–196.
- [15] S.A. Meguid, A.L. Kalamkarov, Asymptotic homogenization of elastic composite materials with a regular structure, *Int. J. Sol. Struct.* 31 (3) (1993) 303–316.
- [16] S. Nemat-Nasser, T. Iwakuma, M. Hejazi, On components with periodic structure, *Mech. Mater.* 1 (1982) 239–267.
- [17] N.A. Nicorovici, R.C. McPhedran, Transport properties of arrays of elliptical cylinders, *Phys. Rev. E* 54 (1996) 1945–1957.
- [18] W.J. Parnell, Coupled thermoelasticity in a composite half-space, *J. Eng. Math.* (2006) (in press).
- [19] V.Z. Parton, B.A. Kudryavtsev, *Engineering Mechanics of Composite Structures*, CRC Press, Boca Raton, FL, 2003.
- [20] C.G. Poulton, A.B. Movchan, R.C. McPhedran, N.A. Nicorovici, Y.A. Antipov, Eigenvalue problems for doubly periodic elastic structures and phononic band gaps, *Proc. R. Soc. Lond. A* 456 (2000) 2543–2559.
- [21] J.W.S. Rayleigh, On the influence of obstacles arranged in rectangular order upon the properties of a medium, *Phil. Mag.* 34 (1892) 481–502.
- [22] R. Rodriguez-Ramos, F.J. Sabina, R. Guinovart-Diaz, J. Bravo-Castillero, Closed-form expressions for the effective coefficients of a fibre-reinforced composite with transversely isotropic constituents – I. Elastic and square symmetry, *Mech. Mater.* 33 (2001) 223–235.
- [23] F.J. Sabina, J. Bravo-Castillero, R. Guinovart-Diaz, R. Rodriguez-Ramos, O.C. Valdiviezo-Mijangos, Overall behaviour of two-dimensional periodic composites, *Int. J. Sol. Struct.* 39 (2002) 483–497.

- [24] F.J. Sabina, J.R. Willis, A simple self consistent analysis of wave propagation in particulate composites, *Wave Mot.* 10 (1988) 127–142.
- [25] I.S. Sokolnikoff, *Mathematical Theory of Elasticity*, 2nd ed., McGraw-Hill, New York, 1956.
- [26] V.K. Varadan, V.V. Varadan, Y-H. Pao, Multiple scattering of elastic waves by cylinders of arbitrary cross section. I. SH waves, *J. Acoust. Soc. Am.* 63 (5) (1978) 1310–1319.
- [27] Y. Yi, S. Park, S. Youn, Asymptotic homogenization of viscoelastic composites with periodic microstructures, *Int. J. Sol. Struct.* 35 (17) (1998) 2039–2055.
- [28] V.V. Zalipaev, C.G. Movchan, A.B. Poulton, R.C. McPhedran, Elastic waves and homogenization in oblique periodic structures, *Proc. R. Soc. Lond. A* 458 (2002) 1887–1912.